The 3rd Japan-China
Joint Conference
on Fluid Machinery
Osaka
April 23-25, 1990

LATERAL FLUID FORCES OF WHIRLING CENTRIFUGAL IMPELLERS WITH VARIOUS GEOMETRIES

H. Ohashi H. Imai
University of Tokyo

A. Sakurai J. Nishihama
Kobe Steel, Ltd. Asahi Glass Co.

SUMMARY

Fluid forces on a rotating centrifugal impeller in whirling motion have a strong influence on the rotordynamic stability of the shaft system. Experiments have been conducted for the cases in which a two- or three-dimensional impeller rotates and whirls on a circular orbit in a vaneless or vaned diffuser. The measured forces are divided into components parallel and normal to the orbit and the normalized force components are plotted against the ratio of whirl speed to rotational speed.

The result indicates that the whirling fluid forces are affected by the geometries of impeller and diffuser. Comparisons are made between two- and three-dimensional impellers and also between vaneless and vaned diffusers. The influence of clearance between casing and front shroud of impeller is also investigated. The whirling fluid forces exert under certain conditions a strong excitation to the shaft vibration.

1. Introduction

For the rotordynamic stability analysis of a turbopump, for example, it is necessary to estimate the fluiddynamic forces acting on each element of the rotor such as journal bearing, wear ring, throttle bushing, balance piston and centrifugal impeller. Many studies have been done for fluid forces on bearings and annular seals but few for forces on impellers, even though they are the principal components of the rotor.

The fluid forces of the interest in the rotordynamic analyses are not the steady forces such as radial and axial thrust, but the unsteady forces which are induced directly by the oscillatory motion of the impeller. When a rotating shaft with a centrifugal impeller whirls as shown in Fig. 1, the impeller motion is the resultant of the whirl of the shaft center and the rotation of the shaft itself. The unsteady flow induced by this whirl motion applies a certain fluid force to the impeller. Since only forces normal to the shaft center give influence on the shaft vibration in a bending mode, our interests are also restricted to the normal component called lateral force.

The bending mode vibration of a rotating shaft typically appears as a whirling motion with an elliptical orbit. If we consider the simple case of a circular orbit, the plane motion of the impeller is illustrated in Fig. 2.

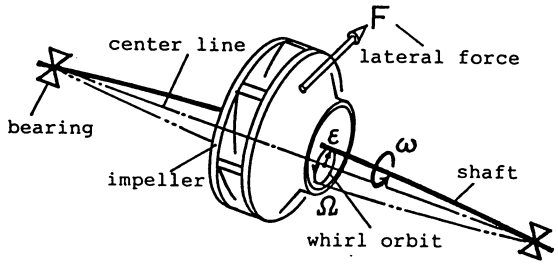

Fig. 1 Centrifugal impeller in whirl motion

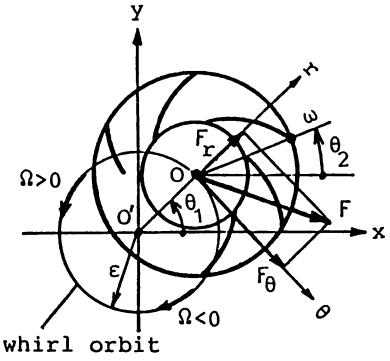

Fig. 2 Force components

The impeller rotates counterclockwise with angular speed ω around its center O, which revolves with angular speed Ω around its absolute center O' along a circular orbit with eccentricity ε. Positive whirl occurs, when the shaft whirls in the same direction as its rotation, and negative whirl in the opposite direction.

The lateral fluid force on the impeller, **F**, is the one which is caused exclusively by the whirling motion. Therefore, any steady fluid forces, which may be caused either by azimuthally asymmetric configuration of surrounding casing or by misalignment of impeller center, are subtracted from the present consideration. The unsteady lateral force is further divided into radial and tangential components, F_r and F_θ, relative to the orbit as shown in Fig. 2.

The radial force component F_r applies a bending moment to the shaft and influences the natural frequency. The tangential force F_θ acts parallel to the motion of the shaft and thus transfers kinetic energy to the whirling rotor. In positive whirl, a positive F_θ (working opposite to the whirl motion) dissipates kinetic energy and exerts a stabilizing or damping effect, while a negative F_θ exerts a destabilizing or excitatory effect. In negative whirl these effects are reversed. When the tangential force becomes excitatory and feeds more kinetic energy to the whirling shaft than it damps out, a severe impeller-induced self-excitation or an impeller whip may occur. From the viewpoint of rotordynamic instability, tangential component has the primary significance.

The lateral fluid forces acting on a two-dimensional (2-D) centrifugal impeller installed in a vaneless diffuser (the most fundamental configuration of a pump) was studied first by the authors experimentally as well as theoretically and the result was reported in references [1,2]. The test apparatus for forced whirling motion was then replaced by a new setup [3] and the studies were further conducted for three-dimensional (3-D) impellers (models of boiler feed pumps) installed in vaneless or vaned diffuser. As an additional parameter survey, the influence of clearance gap between casing wall and front shroud of impeller on the whirling fluid forces was also investigated.

From these experiments following results are summarized in the present paper.

1) Comparison of lateral fluid forces on 2-D and 3-D impellers in vaneless diffuser.
2) Comparison of lateral fluid forces on 3-D impeller in vaneless and vaned diffuser.
3) Comparison of lateral fluid forces on 3-D impeller for various clearance configurations between casing and front shroud.
4) Lateral fluid forces on 3-D impeller in vaned diffuser when rotating stall occurs in diffuser at low discharge.

Similar experimental studies of fluid forces on whirling centrifugal impellers have been conducted at California Institute of Technology [4,5], Sulzer Brothers, Ltd. [6,7] and Mitsubishi Heavy Industries, Ltd. [8]. All measured forces showed the same general tendency qualitatively, however, the magnitude of the forces proved to be very sensitive to the gap between casing and impeller shrouds. The zone of instability, where the fluid forces excite the shaft vibration, was also dependent to the design details of impeller and diffuser.

2. Test facility

The test facility is virtually a single-stage, vertical shaft, centrifugal pump. The overall test setup is illustrated in Fig. 3, which has been fundamentally unchanged since the start of this study. The new apparatus for forced whirling motion is illustrated in Fig. 4. The section view of Fig. 5 illustrates an example of impeller installation in the casing, in this case a 3-D impeller in a vaned diffuser. The experiments on 2-D impellers are done principally for the comparison with theory, while those on 3-D impellers for obtaining whirling force data of impellers in practical application.

Lateral fluid forces on the impeller are measured by the reaction to the lower bearing. The outer race of the bearing is attached to the non-rotating intermediate sleeve by four load cells arranged with 90 degree angle difference (x- and y- direction). The load cells move, therefore, only translatorily on the orbit and keep their direction unchanged. This feature makes the force measurement simple and reliable. The phase angles of whirl and rotation, θ_1 and θ_2 (see Fig. 2), are detected by encoders attached to eccentric sleeve and pump shaft. The rotational speed of the impeller ω is kept constant, while the whirl speed Ω is varied from negative to positive to cover required range of whirl speed ratio Ω/ω. Impeller torque is measured by torque meter installed between motor and flexible coupling.

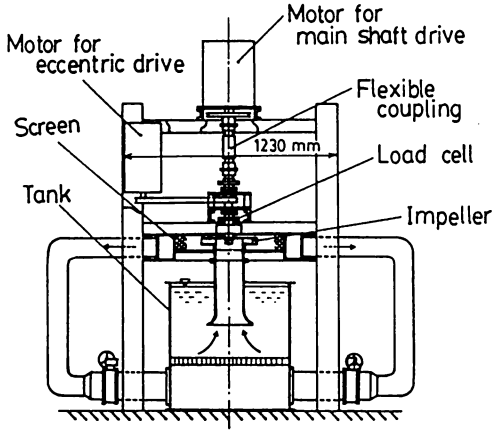

Fig. 3 Test setup

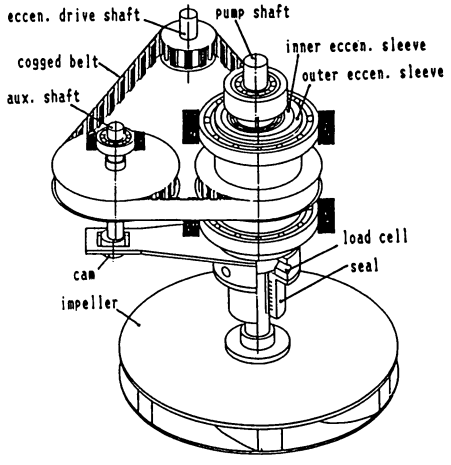

Fig. 4 Apparatus for forced whirl

3. Data presentation

The data acquisition and evaluation were made fundamentally in the same way as described in the previous reports [2,3]. The fluid force $\mathbf{F}(\theta_1,\theta_2)$ is divided into radial and tangential components, F_r and F_θ, as illustrated in Fig. 2. The average forces on the orbit, $\overline{F}_r$ and $\overline{F}_\theta$, are then normalized by the equations;

$$f_r = \bar{F}_r / M\varepsilon\omega^2, \quad f_\theta = \bar{F}_\theta / M\varepsilon\omega^2 \quad \cdots\cdots\cdots\cdots\cdots\cdots\cdots\cdots\cdots\cdots\cdots\cdots(1)$$

where the reference mass $M=\rho\pi r_2^2 b$, ε = eccentricity, ρ = fluid density, r_2 = outer radius and b = impeller exit width. The characteristics of whirling fluid forces will be presented in diagrams, in which normalized radial and tangential force components, f_r and f_θ, are plotted against whirl speed ratio Ω/ω for various discharge conditions from shut-off to full flow.

In the comparison of normalized fluid forces on 2-D and 3-D impellers, the following difference must be kept in mind.

1) For 2-D impellers, fluid forces acting on impeller blades, excluding all other fluid forces on front and back shrouds, impeller hub, etc. are normalized by $M\varepsilon\omega^2$, where b of the reference mass M is the exit width of impeller blades only. Reference mass is therefore the mass of fluid in the volume enveloped by the rotating impeller blades.

2) For 3-D impellers, fluid forces acting on the whole impeller, blades as well as shrouds and hub, are normalized by the quantity $M\varepsilon\omega^2$, where b is the total exit width of the impeller, that is, blade width plus width of two shrouds.

The former definition is convenient for comparing the experimental result with the theoretical one. The latter is for the convenience of practical application, since the fluid forces on impeller blades and shrouds have the same significance on the rotordynamic behavior of the rotating system.

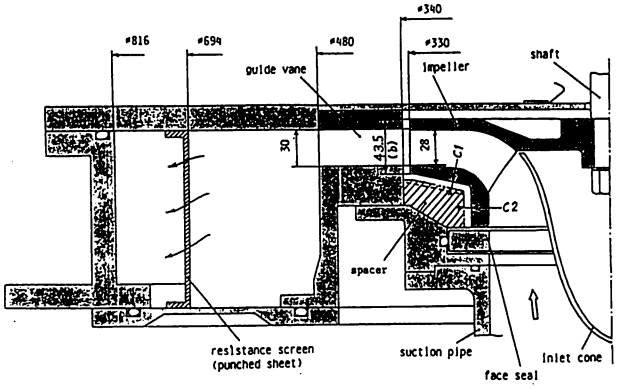

Fig. 5 Impeller and casing configuration of 3-D impeller

4. Fluid forces on 2-D and 3-D impellers in vaneless diffuser

The influence of impeller design, i.e. 2-D impeller with untwisted constant-width blading and 3-D impeller with twisted tapered-width blading, is dealt with in this chapter. The discharge of both impellers is diffused in the succeeding parallel walled vaneless diffuser. The clearance between casing and front shroud of impeller is made sufficiently large and hence the fluiddynamic restriction by surrounding casing is kept small.

Figures 6 (a) and (b) show how normalized tangential and radial force components of 2-D and 3-D impellers vary with whirl speed ratio Ω/ω at design discharge $\phi/\phi_D=1.0$ and at partial discharge $\phi/\phi_D=0.2$, where ϕ_D denotes flow coefficient at design (shock-free entry) condition. As seen from these figures, lateral fluid forces on 3-D impeller is slightly larger than those on 2-D impeller. The most of this difference could be attributed to the fact that 3-D impeller has wider passage width at inlet than at exit and the real volume enveloped by rotating impeller is considerably larger than that of reference mass, $\pi r_2^2 b$. In other words, the forces on 3-D impeller are normalized by relatively smaller quantity compared to the case of 2-D impeller.

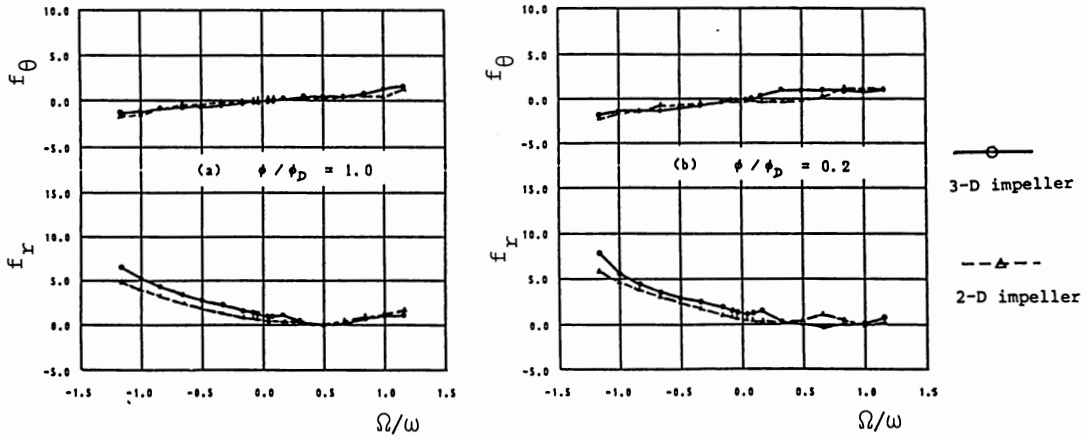

Fig. 6 Fluid forces on 2-D and 3-D impellers in vaneless diffuser

It can be concluded from the experiment that fluid forces on whirling impellers in vaneless diffuser, regardless of 2-D or 3-D, are caused mostly by unsteady fluid forces on whirling impeller blades and coincide with those predicted by theory [1] quantitatively. This is only the case, however, when the impeller is installed in the casing with an ample clearance.

5. Fluid forces on 3-D impeller in vaneless and vaned diffuser.

A 3-D test impeller was installed in the casing as shown in Fig. 5. The eleven guide vanes attached between two parallel walls are removable. With and without guide vanes correspond to the case of vaned and vaneless diffuser, respectively. The mean radial clearance between impeller outer periphery and guide vane inner periphery is 5 mm. When the impeller whirls with an eccentricity of ε=1.5 mm, the clearance varies between 3.5 mm and 6.5 mm. The clearance between casing and front shroud was kept wide (without spacer) throughout this test series. Specifications of 3-D impeller and matching diffuser are given in Table 1.

In the case of vaned diffuser, every time when a trailing edge of 6 impeller blades passes by in the vicinity of a leading edge of 11 guide vanes, a fluiddynamic interaction takes place and the blade receives an impulsive force. The impeller/guide vane interaction can be understood as the sum of these individual impulses. Fig. 7 indicates how fluid force

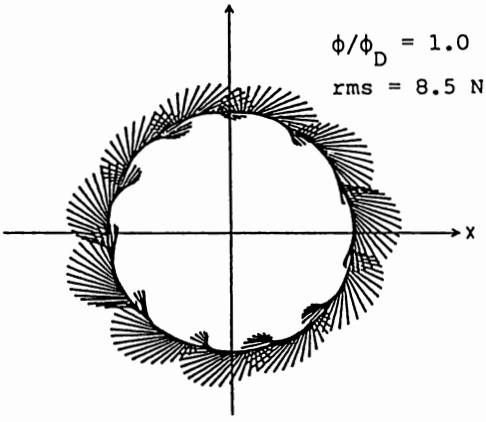

Fig. 7 Impeller/guide vane interaction

Table 1 Specifications

Impeller: Three-dimen., closed type		
Outer blade diameter;	330	mm
Inner blade diameter;	180	mm
Exit blade width;	28	mm
Exit total width;	43.5	mm
Number of blades;	6	
Exit angle to radius;	65.5°	
Mass;	5.6	kg
Diffuser: Parallel walled, vaned type		
Inlet diameter;	340	mm
Exit diameter;	480	mm
Width;	30	mm
Number of vanes;	11	

vectors vary on the orbit when the impeller whirls at $\Omega/\omega=1$ at design flow rate. The observed fine structures of force pattern are all due to the interaction. Such local variation of fluid forces has, however, little meaning from the viewpoint of rotordynamics, since only quantities averaged over an orbit have influence on the stability of the shaft system.

Figures 8 (a) and (b) show the comparison at design discharge $\phi/\phi_D=1.0$ and at partial discharge $\phi/\phi_D=0.2$. It is obvious that the fluid forces on impeller in vaned diffuser are about 50% larger than those in vaneless diffuser. It should be noted that the pressure rise in vaned diffuser is also larger by about 15 to 20% at the same discharge. The general qualitative tendencies of both cases are essentially the same. Despite strong impeller /guide vane interaction as seen in Fig. 7, its influence on orbit-averaged forces remains relatively small.

As seen in Fig. 8 (b), both tangential and radial components indicate a local increase at around $\Omega/\omega=0.1$ to 0.2 at partial discharge. This phenomena are hardly seen near design discharge and are considered as characteristic at partial discharge. The real mechanism of this phenomena is still unknown but observations suggest that a weak rotating stall present in the vaned diffuser at low discharge is trapped and synchronized with the forced whirling motion of the impeller. Propagation speed of rotating stall in a vaned diffuser is usually 10 to 20% of the impeller speed.

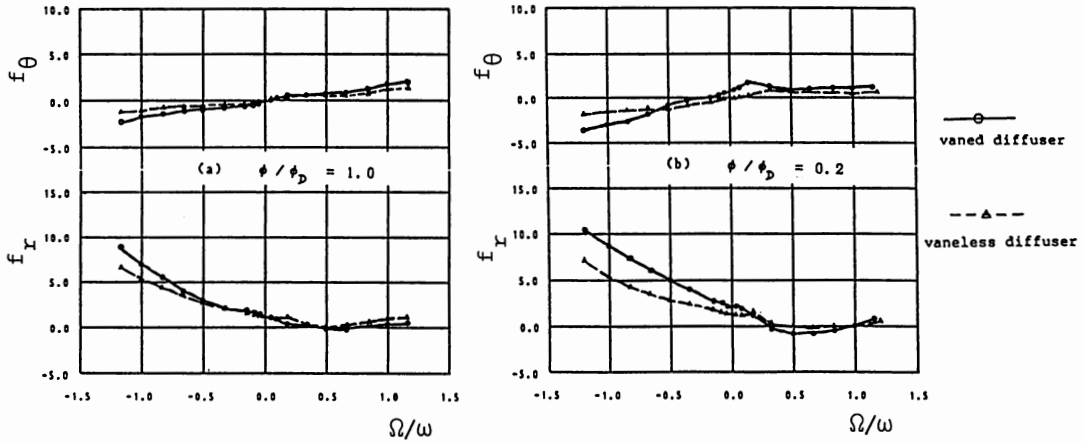

Fig. 8 Fluid forces on 3-D impeller in vaneless and vaned diffuser

6. Fluid forces during rotating stall

An additional test was conducted for a combination of 3-D impeller and vaned diffuser, which have such design parameters that a manifest rotating stall in the diffuser takes place at low discharge. Fig. 9 indicates the result at partial discharge $\phi/\phi_D=0.2$. The violent change of tangential and radial components at very low whirl speed ratio, $\Omega/\omega=0$ to 0.2, suggests that a synchronization of stall zone and whirl motion may occur at very low whirl speed ratio, where the rotational speeds of eccentricity and stall zone are very close.

The large negative tangential force at very low whirl speed ratio indicates that the whirling fluid force exerts a negative damping to the shaft, i.e. it excites shaft vibration. In the case of multistage pumps, the stall cell of every stage may rotate in the same phase as that of shaft eccentricity, thus resulting in a synchronization of whole stall cells. This mechanism can induce a strong vibration of the shaft. A part of shaft vibration problems of multistage centrifugal pumps at partial discharge, experienced occasionally in the past, could be attributed to this synchronization phenomena.

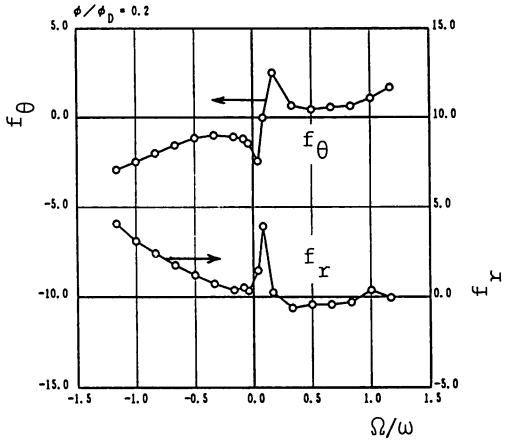

Fig. 9 Fluid forces on 3-D impeller during rotating stall in diffuser

7. Influence of clearance between casing and front shroud

The influence of clearance between casing and front shroud of impeller on whirling fluid forces is dealt with in this chapter. Tests were conducted for 3-D impeller in three cases (see Fig. 5); (a) without spacer (original layout), (b) with spacer to block dead space, C_1=2.7 mm and C_2=3.0 mm, (c) with grooved spacer, that is, spacer with 24 radial grooves with 10 mm width and 5 mm depth on the surface facing to the front shroud.

The result obtained at design discharge is summarized in Fig. 10. As the clearance between casing and impeller shroud gets smaller and thus the restrictive effect of fluid contained in the narrow gap becomes greater, the fluid forces on the front shroud of the whirling impeller increases obviously. This results in the increase of radial component and the decrease of tangential one. Narrower clearance leads definitely to the expansion of whirl excitation range at positive whirl, where tangential component takes negative value.

The grooves on the spacer surface, which are expected to brake the rotation of fluid in the gap, resulted in the increase of tangential component to positive direction, thus reducing the range of whirl excitation at positive whirl.

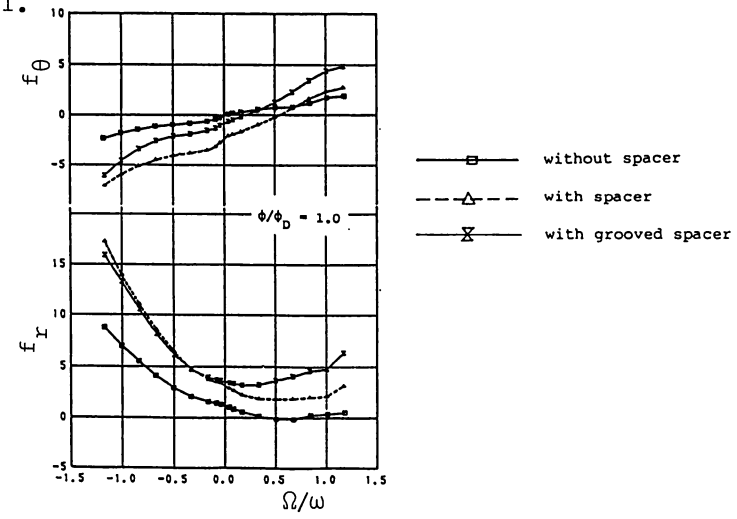

Fig. 10 Influence of clearance configuration on fluid forces

8. Conclusions

Fluid forces on whirling centrifugal impellers are studied experimentally for various configurations of impeller and diffuser. The results obtained are summarized as follows:

1) Comparison of fluid forces on 2-D and 3-D impellers whirling in a vaneless diffuser indicated no significant difference.

2) Fluid forces on 3-D impeller whirling in a vaned diffuser were about 50% larger than those in vaneless diffuser, partly due to the interaction between impeller blades and guide vanes and partly due to the increased pressure rise.

3) If once a rotating stall occurs in the vaned diffuser, there exists the possibility that the propagation of stall is coupled with the whirling motion of the impeller. If such synchronization takes place, strong excitation to the shaft vibration can be introduced.

4) The fluid forces acting on the front shroud of whirling impeller are sensitively affected by the clearance between casing and the shroud. The smaller the clearance, the larger the fluid forces on the whirling shroud. Grooves cut on the casing surface facing to the shroud do augment the damping effect at positive whirl.

Acknowledgment: The present study was supported by the Grant-in-Aid for Developmental Scientific Research from the Ministry of Education, Science and Culture (No. 58850035 and 01850041).

REFERENCES

[1] Shoji, H. and Ohashi, H., Lateral Fluid forces on Whirling Centrifugal Impeller (1st Report: Theory), ASME J. Fluids Eng., 109 (1987), 94.

[2] Ohashi, H. and Shoji, H., ditto (2nd Report: Experiment in Vaneless Diffuser), ditto, 100.

[3] Ohashi, H. et al., Fluid Force Testing Machine for Whirling Centrifugal Impeller, Proc., International Conf. on Rotordynamics, IFToMM/JSME, Tokyo (1986), 643.

[4] Jery, B. et al., Hydrodynamic Impeller Stiffness, Damping and Inertia in the Rotordynamics of Centrifugal Flow Pumps, NASA CP 2338 (1984), 137.

[5] Chamie, D.S. et al., Experimental Measurements of Hydrodynamic Radial Forces and Stiffness Matrices for a Centrifugal Pump-Impeller, ASME J. Fluids Eng., 107 (1985), 307.

[6] Bolleter, U. and Wyss, A., Measurement of Hydrodynamic Interaction Matrices of Boiler Feed Pump Impellers, ASME 85-DET-148 (1985).

[7] Pace, S.E. et al., Rotordynamic Developments for High Speed Multistage Pumps, Proc., 3rd Intern. Pump Symposium, Texas (1986-5), 45.

[8] Yoshida, Y. and Tsujimoto, Y., An Experimental Study of Fluid Forces on a Centrifugal Impeller Rotating and Whirling in a Volute Casing, Trans. JSME, 54-505 (1988), 2275 (in Japanese).